PhLAM Physique des Lasers Atomes et Molécules

Université de Lille

Design and realization of a ^{41}K Bose-Einstein condensate experiment to study the many-body atomic kicked rotor model

Presented by :
Charbel CHERFAN

Postdoctoral fellow on the cold atom gyroscope experiment

SYRTE seminar

February 3, 2022

1. Theoretical background

Kicked rotor (KR)

Kicked rotor (KR)

- Laser cooled atoms exposed to a pulsed standing wave :

$$H = \frac{P^2}{2} + K\cos\theta \sum_n \delta(t-n)$$

Kicked rotor (KR)

- Laser cooled atoms exposed to a pulsed standing wave :

$$H = \frac{P^2}{2} + K \cos\theta \sum_n \delta(t-n)$$

- Classical KR : diffusive motion in phase space
- Quantum KR (QKR) : Exponential localization of the wave function, signature of the dynamical localization (DL)

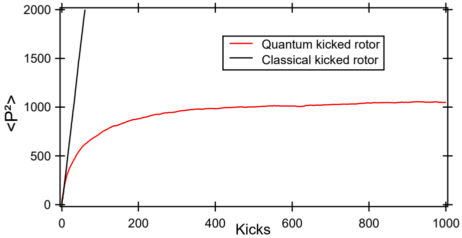

Equivalence with the 1D Anderson localization

Equivalence with the 1D Anderson localization

- The DL strongly evokes Anderson localization

Equivalence with the 1D Anderson localization

- The DL strongly evokes Anderson localization
- The existence of exponentially-localized eigenstates in space
- The existence of a phase transition between delocalized ("metal") and localized ("insulator") phases in three dimensions

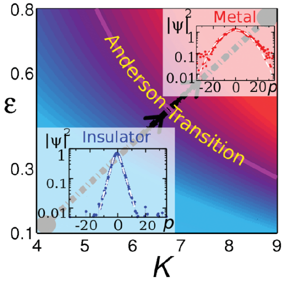

Equivalence with the 1D Anderson localization

- The DL strongly evokes Anderson localization
- The existence of exponentially-localized eigenstates in space
- The existence of a phase transition between delocalized (“metal”) and localized (“insulator”) phases in three dimensions

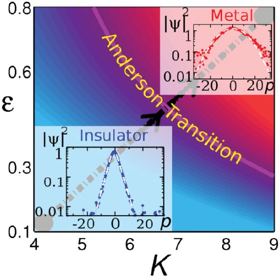

- The KR is used to quantum-simulate Anderson physics

J.Chabé el al., Phys. Rev. Lett. 101, 255702 (2008)

Many-Body physics

Many-Body physics

- Anderson model + interactions : Many-Body localization (MBL)

Many-Body physics

- Anderson model + interactions : Many-Body localization (MBL)
- KR+interactions: ?

Many-Body physics

- Anderson model + interactions : Many-Body localization (MBL)
- KR+interactions: ?

Mean field approximation (Gross-Pitaevskii)

Breakdown of the DL which is replaced by subdiffusion

Shepelyansky, Phys.Rev.Lett. 70, 1787 (1993)

Cherroret et al., Phys.Rev.Lett. 112, 170603 (2014)

Many-Body physics

- Anderson model + interactions : Many-Body localization (MBL)
- KR+interactions: ?

Mean field approximation (Gross-Pitaevskii)

Breakdown of the DL which is replaced by subdiffusion

Shepelyansky, Phys.Rev.Lett. 70, 1787 (1993)
Cherroret et al., Phys.Rev.Lett. 112, 170603 (2014)

Infinite interaction Tonks regime

Observation of Many-Body Dynamical Localization (MBDL)

Rylands et al., Phys.Rev.Lett. 124, 155302 (2020)
Chicireanu et al., Phys.Rev.A 103, 043314 (2021)
Vuatelet et al., arxiv : 2103.14388 (2021)

Many-Body physics

- Anderson model + interactions : Many-Body localization (MBL)
- KR+interactions: ?

Mean field approximation (Gross-Pitaevskii)

Breakdown of the DL which is replaced by subdiffusion

Shepelyansky, Phys.Rev.Lett. 70, 1787 (1993)
Cherroret et al., Phys.Rev.Lett. 112, 170603 (2014)

Infinite interaction Tonks regime

Observation of Many-Body Dynamical Localization (MBDL)

Rylands et al., Phys.Rev.Lett. 124, 155302 (2020)
Chicireanu et al., Phys.Rev.A 103, 043314 (2021)
Vuatelet et al., arxiv : 2103.14388 (2021)

Global objective:

Construction of a potassium BEC experiment, with controllable interactions

Choice of the potassium

- Control the interactions between atoms in the system via the Feshbach resonances
- ^{7}Li and ^{39}K are the two alkalines that are favorable due to their broadness of resonance and the value of B_0 accessible
- The cooling transitions of the potassium isotope corresponds to half of the wavelength of the Telecom domain

Atome	$B_0(G)$	Δ(G)	a_{bg}/a_0	λ_{D2}(nm)
^{7}Li	736,8	-192.3	-25	670
^{39}K	402,4	-52	-29	767
^{41}K	51,4	-0.3	60	767
^{85}Rb	155,04	10.7	-433	780
^{87} Rb	1007,4	0.21	100	780

2. Construction of the experiment

Atomic structure of ^{41}K

- Very narrow hyperfine structure of the excited state of the D2 transition
- Magneto-optical trap (MOT) temperatures relatively high ($\sim$ mK), therefore unfavorable for condensation
- Using the D1 transition for the gray molasses
- Development of two laser systems, for the two D transitions of potassium

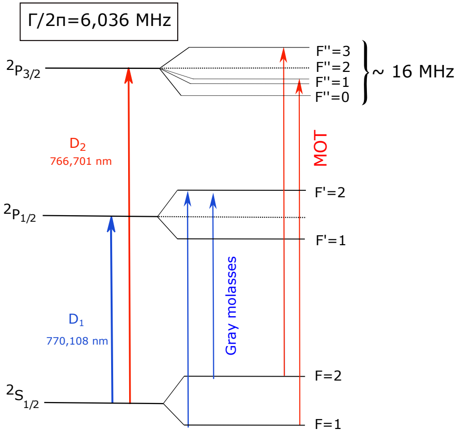

Ultra-high vacuum setup

- Experimental setup composed of two vacuum chambers
- A 2D MOT will be created in the first chamber, which contains the potassium vapor
- This will provide a beam of atoms to the main chamber, in which a 3D MOT will be created

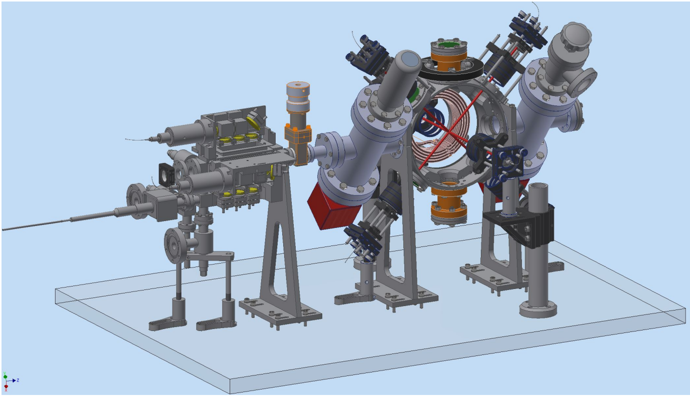

Experimental sequence

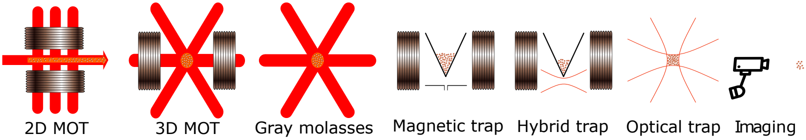

Experimental sequence

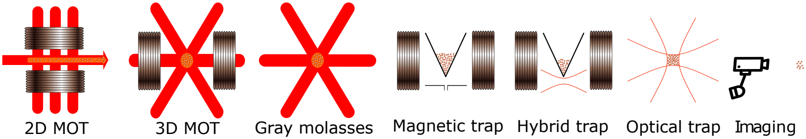

- Accumulation of atoms in the 3D MOT using the D2 line

Experimental sequence

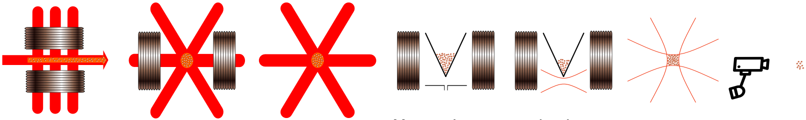

- Accumulation of atoms in the 3D MOT using the D2 line
- Compressed-MOT (CMOT) and sub-Doppler cooling using the D1 line

Experimental sequence

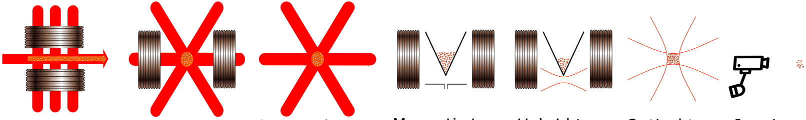

- Accumulation of atoms in the 3D MOT using the D2 line
- Compressed-MOT (CMOT) and sub-Doppler cooling using the D1 line
- Evaporative cooling in conservative traps
  → Magnetic trap and radio-frequency (RF) evaporation
  → Transfer to a magnetic + optical trap (hybrid trap)
  → Transfer to a crossed optical dipole trap

Telecom fibered laser system

Telecom fibered laser system

- Semiconductor laser diodes in external cavities, further amplified with slave diodes or tapered amplifiers(TA)
- Several drawbacks: limited lifetime of TA, poor quality of spatial mode
- Powerful lasers are either too costly or unavailable at the desired wavelength

Telecom fibered laser system

- Semiconductor laser diodes in external cavities, further amplified with slave diodes or tapered amplifiers(TA)
- Several drawbacks: limited lifetime of TA, poor quality of spatial mode
- Powerful lasers are either too costly or unavailable at the desired wavelength
- SHG from the telecommunication band to the NIR
- Laser cooling systems relying on telecom technologies and SHG have been tested in the case of rubidium and potassium

Stern et al., Appl. Opt. 49(16), 3092-3095 (2010)

Telecom fibered D2 laser system

Telecom fibered D2 laser system

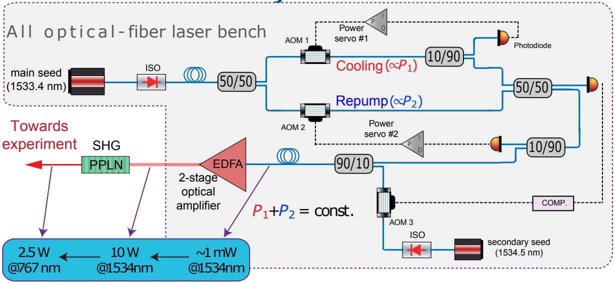

- Generation of the cooling and repumper frequencies before EDFA (Erbium Doped Fiber Amplifier) and SHG (Second Harmonic Generation) in a PPLN crystal (Periodically Poled Lithium Niobate)
- Control of frequencies and relative laser power via fibered acousto-optic modulators (AOM's)
- Generate 2.5 W after frequency doubling in the PPLN crystal

Cherfan et al., Appl. Phys. Lett. 119, 204001 (2021)

Ballast laser

- Both wavelengths are at the band edge of the EDFA
- Ensures an efficient and rapid switch, necessary in later stages of the experiment
- Reduction of the SHG efficiency by optimizing the wavelength of the ballast laser (1534.6 nm)
- Optical power attenuation of $\sim$ 30 dB

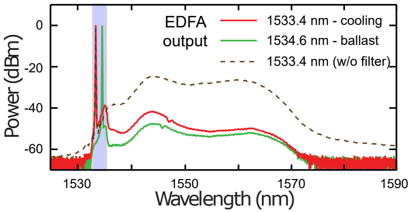

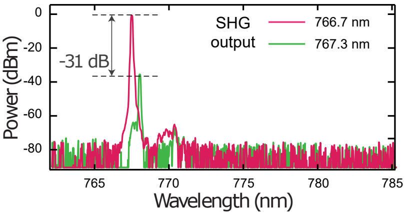

Characterization of the SHG

- Bichromatic beam at the input of the PPLN crystal (after EDFA)
- Generation of the SHG of each component and their sum frequency by the non-linear process
- Spectral line shape of the beatnote spectrum detected on a photo-diode

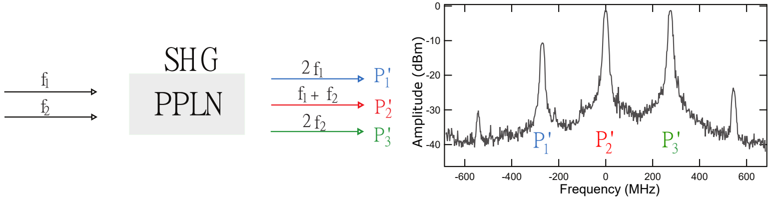

Calibration of the power ratio r

- Spectral characterization of the system to describe the SHG stage
- P_2' and P_3' correspond to the cooling and repumpeur beams respectively
- The calibration is modified for higher powers due to thermal effects in the PPLN crystal

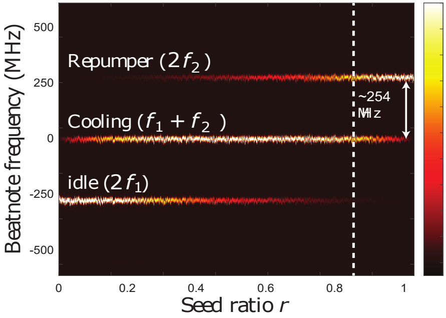

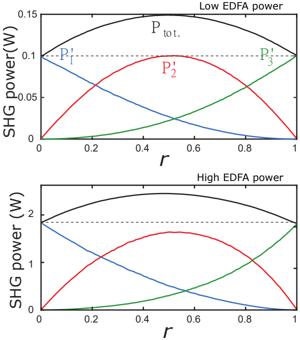

D1 laser system

- Construction of a second laser system, similar to the D2 system, for the D1 transition
- DFB at 1540 nm and another heating temperature for the PPLN crystal
- Better performance than the D2 system with a maximum power of 2.8 W

D1 laser system

- Construction of a second laser system, similar to the D2 system, for the D1 transition
- DFB at 1540 nm and another heating temperature for the PPLN crystal
- Better performance than the D2 system with a maximum power of 2.8 W
- Change in the order of the optical components of the D1 bench compared to the D2 bench

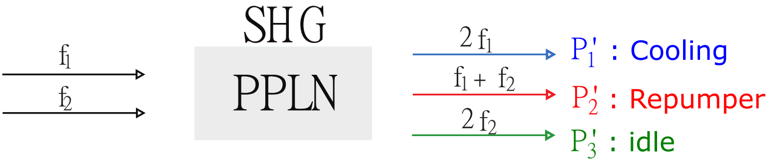

Free space laser system

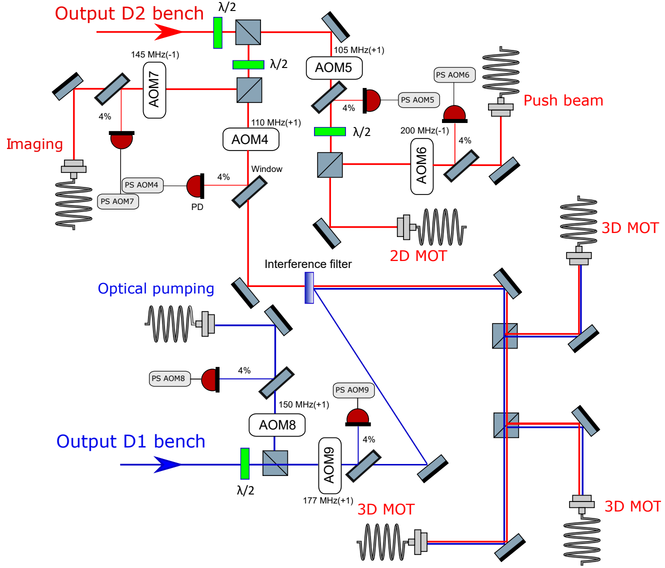

Acetylene based frequency stabilization

Acetylene based frequency stabilization

- We use a ro-vibrational transitions of the acetylene molecule, close to twice the wavelength of the potassium D transitions
- The frequency stabilization can be completely decoupled from the power amplification and SHG stages

Acetylene based frequency stabilization

- We use a ro-vibrational transitions of the acetylene molecule, close to twice the wavelength of the potassium D transitions
- The frequency stabilization can be completely decoupled from the power amplification and SHG stages
- The double of the wavelengths of the potassium D lines (vertical dashed lines) are close to different transitions in the P branch

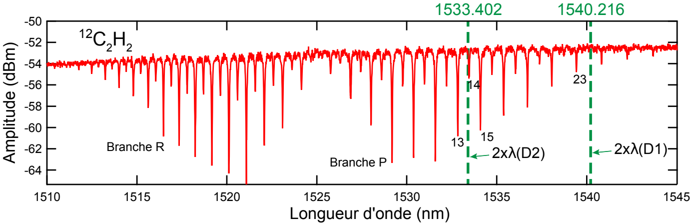

Cherfan et al., Opt. Express 28, 494-502 (2020)

Experimental setup

- Stabilize the frequency of an ultra-narrow line (UNL) laser diode via saturated absorption spectroscopy using an acetylene cell
- Phase-lock the acetylene and the potassium diode lasers, before SHG

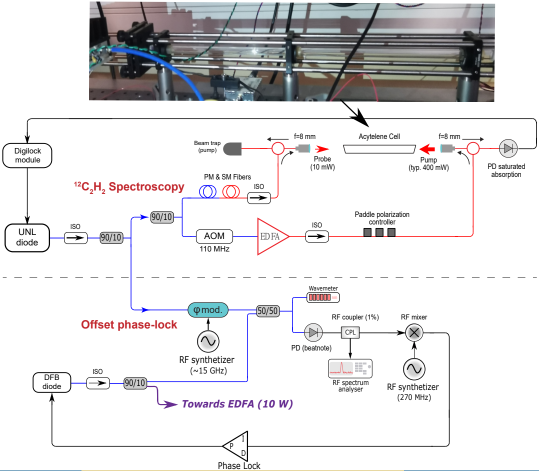

Acetylene saturated absorption spectroscopy

- Observation of two acetylene lines relevant to potassium
- Generation of the error signal for frequency locking of the UNL laser by implementing a modulation transfer scheme
- They feed the PID filters, that generate the correction signal sent to the UNL diode laser

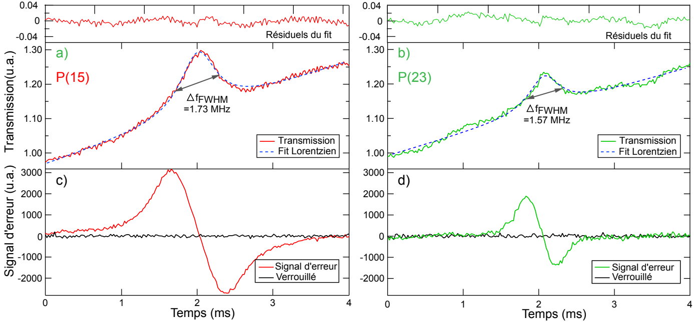

Phase lock

- A phase modulator is implemented after the UNL laser
- Detection of the low-frequency beatnote between the DFB diode (SHG) and the UNL laser (acetylene), via a high-order harmonic of the phase modulator
- Phase-lock of the DFB laser diode to the acetylene-stabilized UNL laser

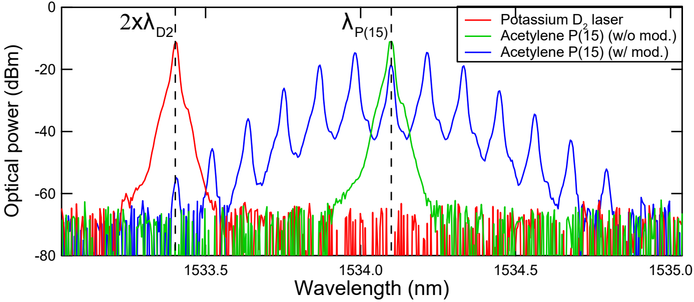

3. Laser cooling

Magneto-optical trapping of the ^{41}K atoms

- Observation of the first 2D MOT and 3D MOT in 2019
- Optimization of the MOT parameters thanks to the versatility of our laser system
- We use a weak magnetic field gradient of 5.5 G/cm

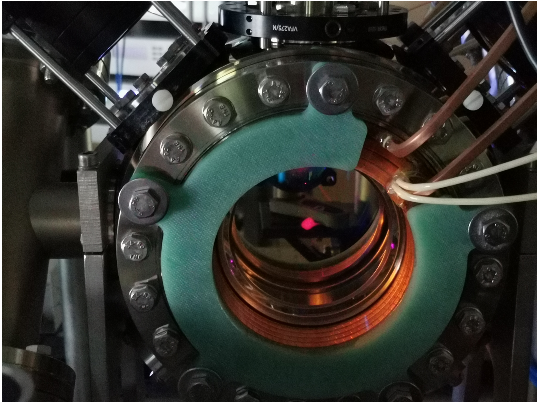

Magneto-optical trapping of the ^{41}K atoms

- The detunings of the cooling and repumper are -5.5 Γ and -4.1 Γ respectively
- We are able to trap up to 3×10^9 atoms of ^{41}K with a loading time of approximately 2.5 s
- 2D plot representing the number of trapped atoms as a function of the fibered AOM's frequencies

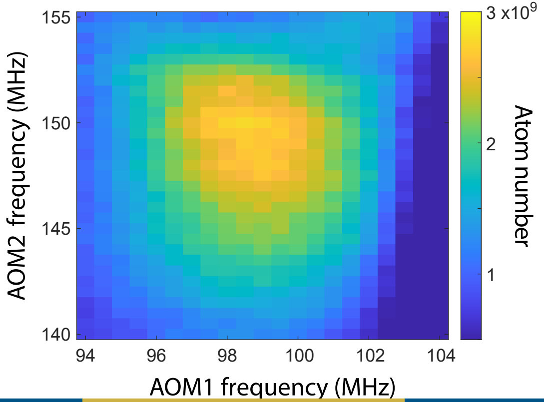

Hybrid compressed MOT

Hybrid compressed MOT

- Hybrid scheme: cooling of the D1 transition + repumper of the D2 transition
- A gray molasses type cooling occurs for the D1 light

Hybrid compressed MOT

- Hybrid scheme: cooling of the D1 transition + repumper of the D2 transition
- A gray molasses type cooling occurs for the D1 light
- Study of the density and temperature as a function of the magnetic field gradient at the end of the compression ramp
- Compromise to be made, between temperature (low) and density (high)

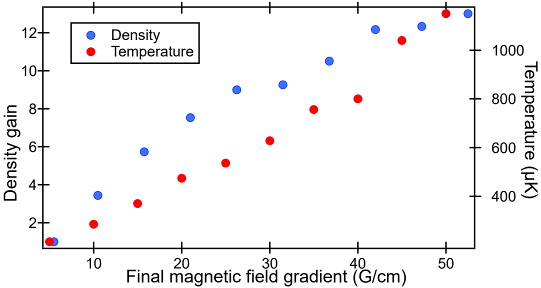

Gray molasses

Gray molasses

- Using the cooling and the repumper of the D1 transition
- Rely on a Λ level scheme where the detuning $\delta = 0$ provides the optimum parameters
- Capture of CMOT atoms using the maximum available power
- Power ramping to further cool the atoms down to 16 μK

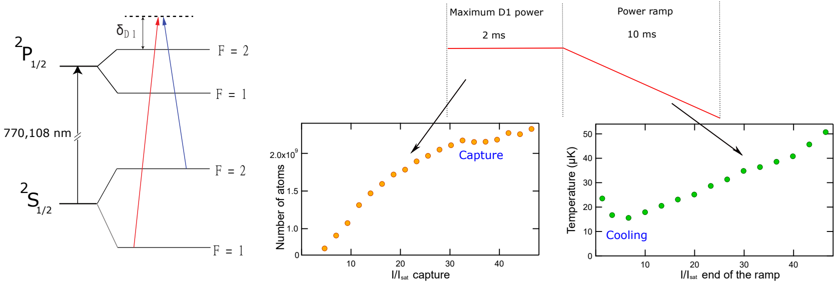

4. BEC of ^{41}K

Conservative traps

Conservative traps

- **Quadrupole magnetic traps:**

Conservative traps

- **Quadrupole magnetic traps:**
  1. Advantages:
  → Large capture volume
  → Unchanged trap depth during the RF evaporation

Conservative traps

- **Quadrupole magnetic traps:**
  1. Advantages:
  → Large capture volume
  → Unchanged trap depth during the RF evaporation
  2. Disadvantages:
  → Long evaporation cooling
  → Majorana losses

Conservative traps

- **Quadrupole magnetic traps:**
  1. Advantages:
  → Large capture volume
  → Unchanged trap depth during the RF evaporation
  2. Disadvantages:
  → Long evaporation cooling
  → Majorana losses
- **Optical dipole traps:**

Conservative traps

- **Quadrupole magnetic traps:**
  1. Advantages:
  → Large capture volume
  → Unchanged trap depth during the RF evaporation
  2. Disadvantages:
  → Long evaporation cooling
  → Majorana losses
- **Optical dipole traps:**
  1. Advantages:
  → Application of a uniform magnetic field
  → Easier to set up
  → Faster evaporation

Conservative traps

- **Quadrupole magnetic traps:**
  1. Advantages:
  → Large capture volume
  → Unchanged trap depth during the RF evaporation
  2. Disadvantages:
  → Long evaporation cooling
  → Majorana losses
- **Optical dipole traps:**
  1. Advantages:
  → Application of a uniform magnetic field
  → Easier to set up
  → Faster evaporation
  2. Disadvantages:
  → Low capture volume
  → Changing the trap depth during the optical evaporation

Hybrid trap

Hybrid trap

- Combines the advantages of magnetic and optical traps

Hybrid trap

- Combines the advantages of magnetic and optical traps
- Use of a magnetic trap evaporated by RF to charge this trap

Hybrid trap

- Combines the advantages of magnetic and optical traps
- Use of a magnetic trap evaporated by RF to charge this trap
- Quadrupole magnetic trap + optical trap shifted vertically from the magnetic field minimum

Hybrid trap

- Combines the advantages of magnetic and optical traps
- Use of a magnetic trap evaporated by RF to charge this trap
- Quadrupole magnetic trap + optical trap shifted vertically from the magnetic field minimum
- Advantages:
  $\rightarrow$ Large depth and capture volume
  $\rightarrow$ Eliminates the need for a high power laser
  $\rightarrow$ Gravity compensation due to magnetic confinement
  $\rightarrow$ Eliminates the problem of Majorana losses

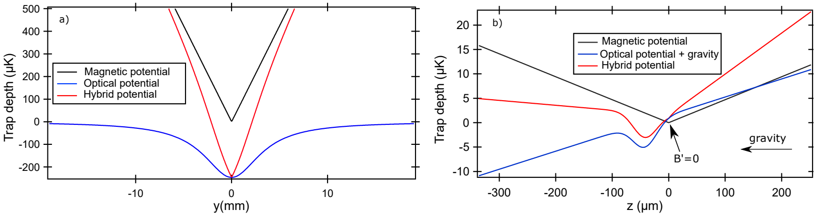

Optical dipole trap

Optical dipole trap

- Construction of an original laser system using an EDFA for the optical dipole trap
- We use fibered AOM's and dichroic mirrors (DM) in free space

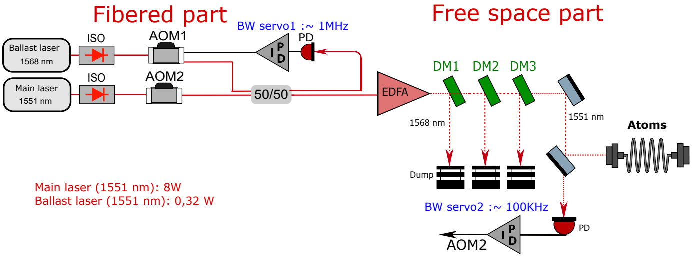

Cherfan et al., Multi-wavelength EDFA-based optical dipole trapping for ultracold atoms, In preparation

Optical dipole trap

- Power characterization of the DM's
- Power control of the trap beam via the power servo 2
- Achievement of a very good extinction ratio ($\sim 10^{-5}$)
- Trap depth of 246 μK at the atomic level

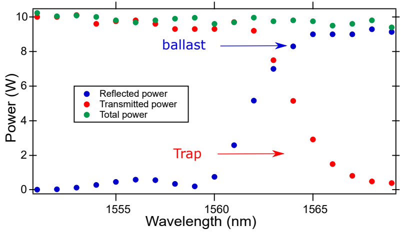

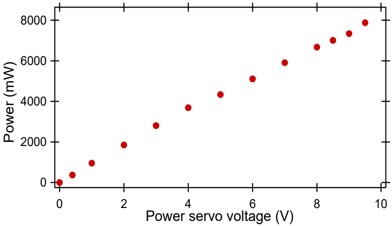

Magnetic trap and RF evaporation

Magnetic trap and RF evaporation

- All the atoms are optically pumped to the $|F = 2, m_F = 2\rangle$ state by using the D1 transition
- We capture 1×10^9 atoms at a temperature of 200 μK
- We keep 40×10^6 atoms at a temperature of 40 μK after the RF evaporation

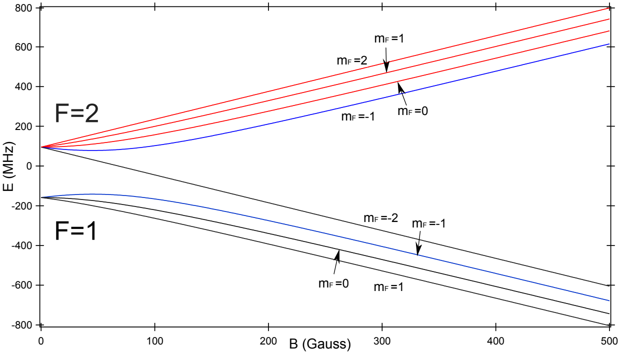

Transfer to the hybrid trap

Transfer to the hybrid trap

- Transfer of the atoms from the quadrupole trap to a combined magnetic and optical trap
- Adiabatic decompression of the magnetic field gradient during two seconds
- We keep 4.2×10^6 atoms at a temperature of 24 μK

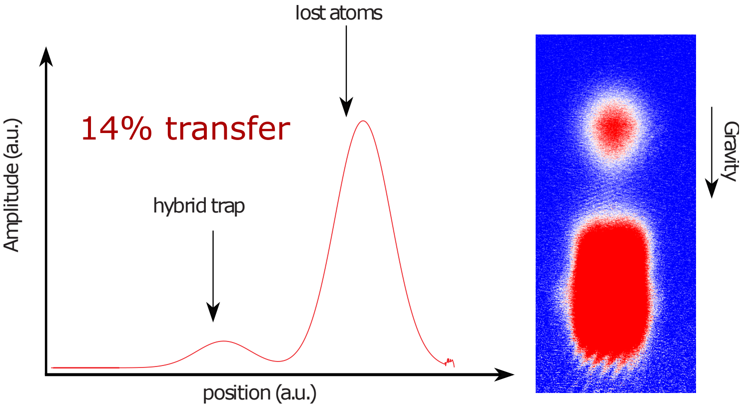

First BEC in the hybrid trap

- We reduce the power of the optical dipole trap beam

First BEC in the hybrid trap

- We reduce the power of the optical dipole trap beam
- At T=300 nK, a bimodal distribution appeared by absorption imaging
- By further evaporation, a near pure BEC with N=60 000 atoms of ^{41}K was observed

Bimodal distribution at T=300 nK

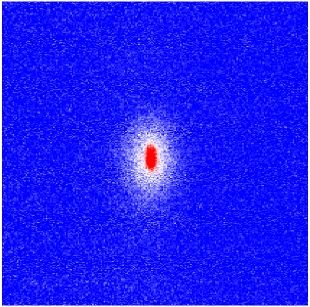

Transfer to the crossed optical dipole trap

Transfer to the crossed optical dipole trap

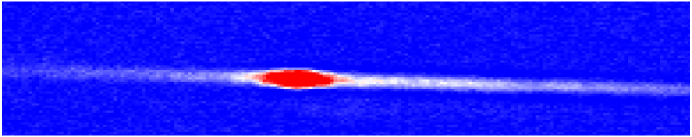

- We transfer the atoms from the hybrid trap to the crossed optical trap before the condensation threshold
- We benefit from the un-doubled IR power of the D1 bench for the additional optical trap beam
- It has a power of 2.43 W, a waist of 118 μm at 1540 nm
- We measure 8 $\times 10^5$ atoms at 1.16 μK

BEC in the crossed optical trap

- We maintain the same trap depth for both beams during evaporation
- We observe a pure BEC with 2×10^5 atoms
- The crossed optical trap is more confining than the hybrid trap

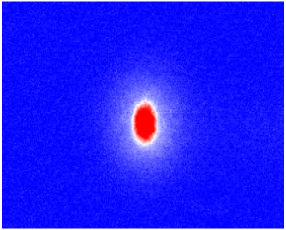

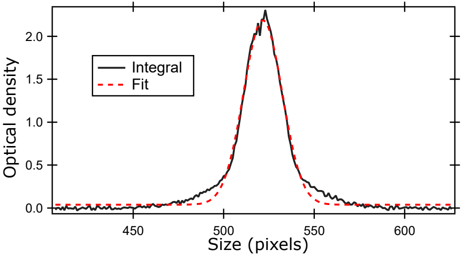

5. Conclusion and outlook

Conclusion

- Design and realization of a new fibered TELECOM system for laser cooling for the D1 and D2 transitions
- Observation of the first 2D MOT and 3D MOT in 2019
- Development of an original laser system for optical dipole trapping
- Observation of the first BEC in a hybrid trap in 2021
- Condensation in a pure optical trap with 2×10^5 atoms
- Control of the interactions via Feshbach resonances

Experimental observation of a Feshbach resonance

- Experimental observation of a Feshbach resonance in the $|F = 1, m_F = -1\rangle$ state
- B_0= 51.4 G and with a resonance width of 0.4 G
- Calibration of the magnetic field of the experiment
- Validation of the experimental system developed in this thesis

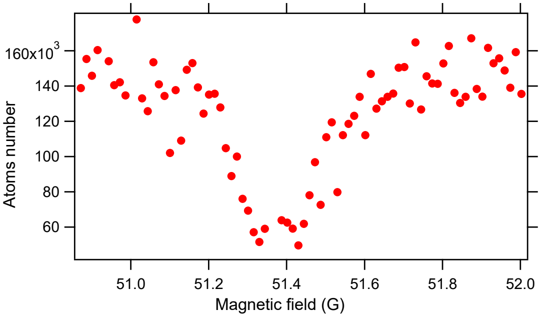

Outlook

- Setting up the pulsed laser to study the QKR model

- QKR with interactions :
  $\rightarrow$ Observation of the subdiffusion in the mean field regime
  $\rightarrow$ Observation and study of the MDBL in the Tonks-Girardeau regime

- QKR without interactions : Observation and study of the 4D Anderson transition

Publications

- C. Cherfan et al., "Acetylene-based frequency stabilization of a laser system for potassium laser cooling.," Opt. Express 28, 494-502 (2020)
- C. Cherfan et al., " Telecom fibered laser system for potassium laser cooling", Appl. Phys. Lett.119, 204001 (2021)
- C. cherfan et al., "Fiber-based acetylene frequency stabilization of a potassium laser cooling system," in Frontiers in Optics + Laser Science 2021, paper FM1A.3
- C. Cherfan et al., " Multi-wavelength EDFA-based optical dipole trapping for ultracold atoms", In preparation.

- **PhD students :** Maxime Denis, Farid Madani, Sammir Zemmouri

- **Post-doc :** Isam Manai

- **Permanent members :** Radu Chicireanu, Jean-François Clément, Denis Bacquet, Pascal Szriftgiser, Jean-Claude Garreau, Michel Gamot, Hervé Damart et Gauthier Dekyndt

Thank you for you attention